

Characterisation and Entrapment of Ladle Glazes in the Molten Steel.

S Riaz^{a)}, A.Cederlund-Losenborg^{b)}, K C Mills^{a)} and K. Bain^{c)}

a): Department of Materials, Imperial College of STM, London, SW7 2BP, UK

b): Department of Theoretical Metallurgy, (KTH), Stockholm, S-10044 Sweden.

c): Corus Group Teesside Technology Centre, Grangetown, Middlesbrough, TS6 6UB, UK.

Abstract

When a ladle is drained the molten slag (protecting the metal) coats the refractory with a layer of slag or glaze. This glaze is a source of inclusions in the next cast. This paper shows that some of the inclusions in the final product originate from this glaze. The effect of the flow of slag down the refractory and also into the pores of the refractory have been studied. Some characterisation of the slags has been carried out. It has been shown that slag penetration into refractory can be minimised by the application of an electric potential of –1 volt between the refractory and the slag.

Introduction

Ladle glazes are formed by the coating of the ladle refractory with a thin layer of slag during the draining of the steel. When the next cast of steel is poured into the ladle this glaze is detached and becomes a source of inclusions in this cast [1-6]. It is interesting to note that despite the current, global drive to produce ever-cleaner steels there is little known about the formation of glazes and how they finish up as inclusions in the steel. This project was initiated to improve our understanding of ladle glazes.

When the metal is drained from the ladle, the descending slag layer comes into contact with the refractory lining of the ladle and adheres to it (forming a *descending slag layer*) [5]. This is shown in Figure 1. The slag also penetrates into the pores of the refractory and forms a “*penetrated slag layer*” [5]. When the metal has drained from the ladle, the ladle is tilted and the slag poured off [5]. This results in the formation of a ridge of slag about 5mm thick in a circumferential position, which is known as the *tilted slag layer*. When the ladle is refilled with molten metal, it is assumed that the adhered slag layer becomes molten, is detached and entrained in the metal flow. Whilst in the metal flow the slag will react with the metal resulting in modification of the inclusion composition. Furthermore, the slag which has penetrated into the pores of the refractory can react with the refractory to produce a modified refractory material. This layer has different properties (e.g. thermal expansion coefficient) to the refractory may produce “spalling” during subsequent cooling and heating of the ladle. The depth of penetrated slag layer and the thickness of the adhered slag layer are important because they may control the quantity of the inclusions entrained in the molten metal.

There is no direct evidence that these adhered glazes are a source of inclusions in the final product. However, there is an indirect anecdotal evidence that a clean cast can only be obtained by using a new ladle. Thus it was one of the objectives of the present investigation to establish that inclusions in the cast originated from these glazes.

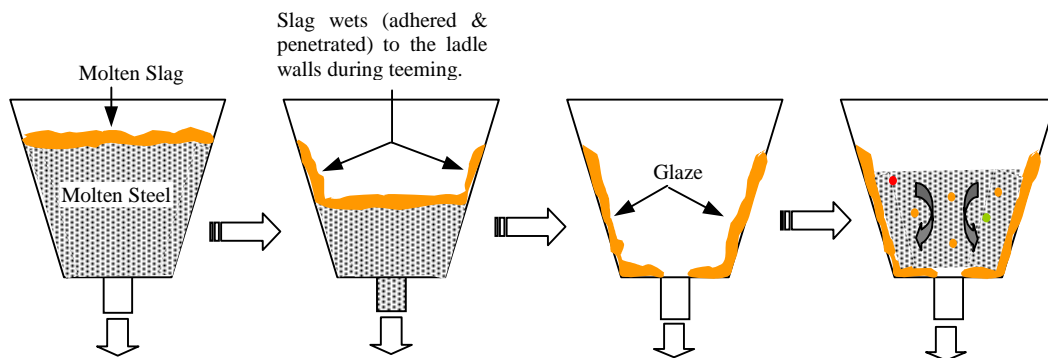


Figure 1: Schematic illustrating the formation of a glaze on the ladle wall.

In this investigation experiments have been carried out to improve our knowledge of the following:

- (i) The mechanisms responsible for the formation of glazes and the infiltration of slag into the refractory.
- (ii) The mechanism and the factors affecting detachment of the glaze from the refractory
- (iii) Glazes as a source of inclusions

These are described below.

2 Formation of Glazes

Several studies have been carried out on glazes to gain an understanding of the mechanisms responsible for the formation of glazes and the infiltration of slag into the refractory.

2.1 Pilot plant studies

A small 4 tonne pilot plant ladle, in which a short sequence of representative grades of steel were made, was very carefully dismantled to examine the effect of repeated use of the ladle on the ladle glaze. The ladle, which was lined with MgO-3%C bricks with a MgO rammable base, was allowed to cool to room temperature after each cast and pre-heated for each subsequent cast. Figure 2a-b shows one of the vertical sections taken through the ladle along with a schematic representation of the section. It is clear from the section profile that both erosion and deposition have occurred over the life of the lining. The glaze, towards the bottom of the ladle, exhibits a relatively smooth surface varying between 10 and 15 mm in thickness. At the top of the ladle, however, where larger and, possibly more varied, heat losses occur, the glaze affected region became thicker and more irregular due to the formation of small slag accretions as opposed to what is customarily considered as ladle glaze. Samples were taken from different levels for chemical and microscopic analysis. It was immediately apparent that the clearly defined interface between the slag and the refractory substrate occurred at the decarburized, non-slag infiltrated refractory surface. The strength of the interface varied greatly between extremely weak and very tightly bonded indicating that several factors, including stresses within the bricks, influence the stability of the glaze layer.

The chemical profile down the section, corrected for undissolved refractory, is given in Figure 2c. This clearly shows that in the upper half of the ladle, the glaze composition was reasonably constant; major changes only occurred in the lower regions of the ladle. The compositions in lower part of the ladle show a marked decrease in MgO with a concomitant increase in the contents of other oxides. At the end of tapping the cooling top slag is

concentrated at the bottom prior to tipping the ladle to remove the liquid slag. This extra contact time may have lead to an apparent increase in the (slag/refractory) ratio near the base of the ladle. The sudden increase in MgO in the sample taken from the bottom of the ladle is probably due to the influence of the rammable refractory base lining.

The microstructure of the refractory/glaze surface can be generalised as being made up of four distinct layers:

1. An outer relatively homogeneous slag layer
2. A two phase slag infiltrated layer.
3. A decarburised refractory layer.
4. The normal refractory brick structure.

The outer layer, which varied considerably in thickness over the height of the ladle (0 to 1 mm) is frequently identified as the final slag deposition as the metal-slag interface descends during tapping. However, in the present examination this surface layer increases in spinel ($\text{MgO} \cdot \text{Al}_2\text{O}_3$) content towards the bottom of the ladle. Figure 3 shows SEM element distribution maps (red is high concentration and blue is low) of two samples from different levels in the ladle. In the Figure 3a, the surface layer clearly shows the presence of a $\text{CaO} \cdot \text{SiO}_2$ $\text{MgO} \cdot \text{Al}_2\text{O}_3$ slag. However, the depletion of CaO and SiO_2 just below this surface layer indicates the presence of a thin region of $\text{MgO} \cdot \text{Al}_2\text{O}_3$ forming at the slag-infiltrated brick boundary. At the bottom of the ladle, Figure 3b, the surface layer is now almost completely $\text{MgO} \cdot \text{Al}_2\text{O}_3$. As the last grade of steel through the ladle was aluminium killed, it is suggested that one of two mechanisms of alumina transfer may have occurred a) alumina inclusions from the liquid steel have collected on the wall of the ladle and been assimilated into glaze, or b) aluminium dissolved in the metal has reduced silica in the slag infiltrated brick and in both cases precipitated spinel. The infiltrated slag showed very similar compositions and distributions in all of the samples examined suggesting that the differences in the measured compositions are dominated by the grade of steel and the method by which it is made.

Within the infiltrated layer of several of the samples, and visible as an arc in the Mg frame of Figure 3b were thin films of either continuous MgO or spinel ($\text{MgO} \cdot \text{Al}_2\text{O}_3$), see also Figure 3c. These films have been found in glaze samples taken from operational plant ladles where they can grow to 1-2 mm thick. Although the authors have previously found evidence to suggest that these were originally surface phenomena forming linear features, the present shape and location have yet to be fully understood.

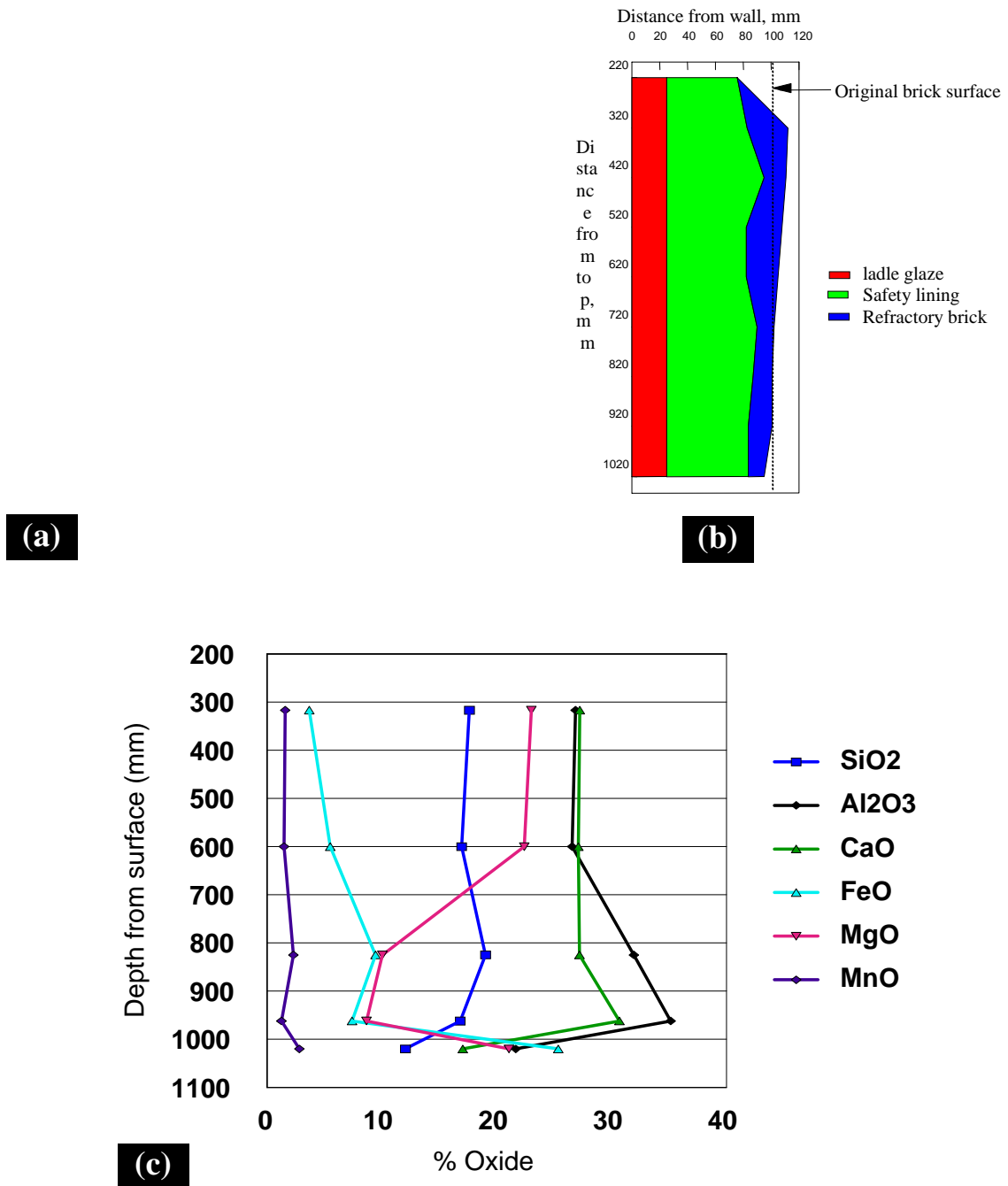
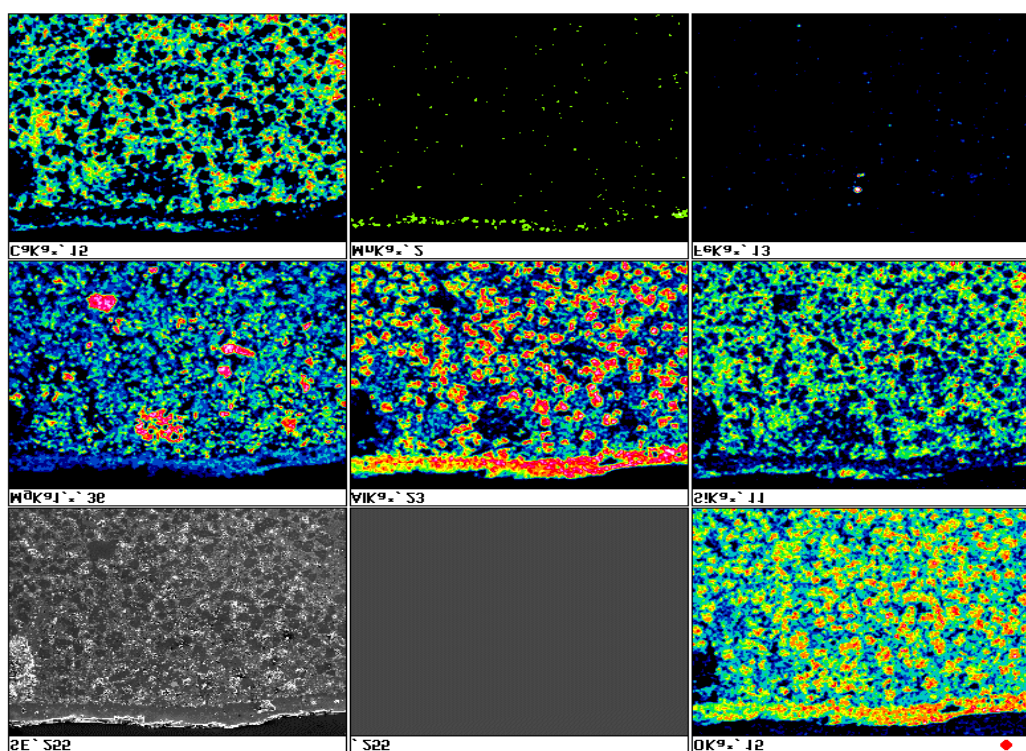
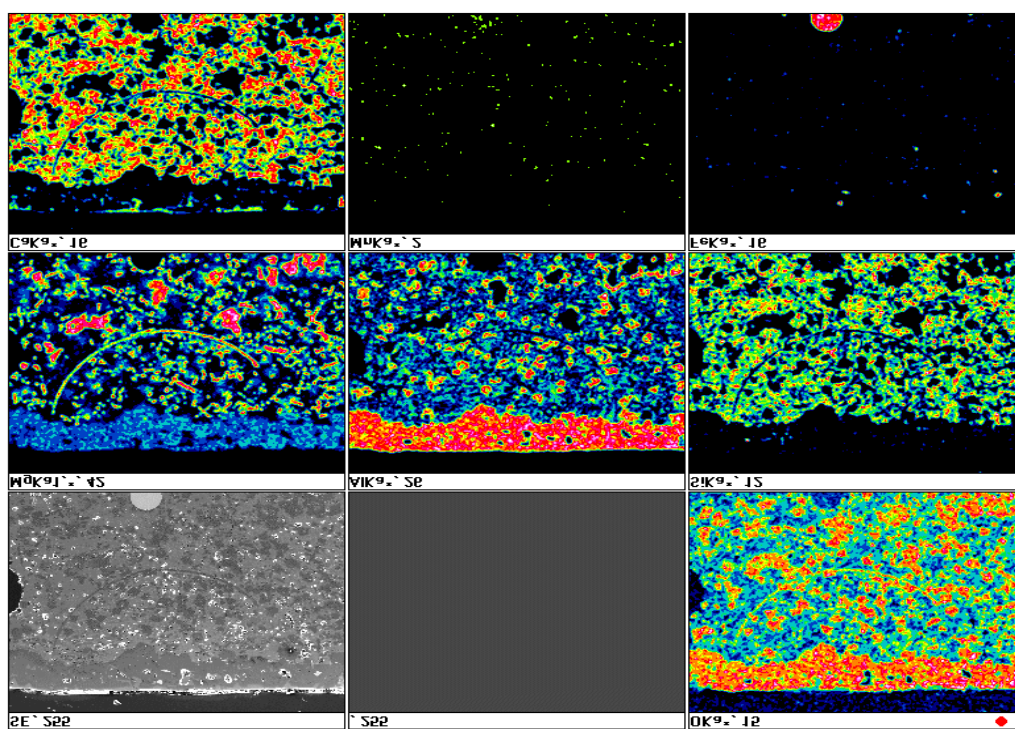


Figure 2: (a-b) - Photograph and profile thickness of the glaze; © - composition as a function of depth from surface.



a)

825mm from top of ladle



b)

1118 mm from top of ladle

Figure 3a-b: SEM element distributions of the surface layers.

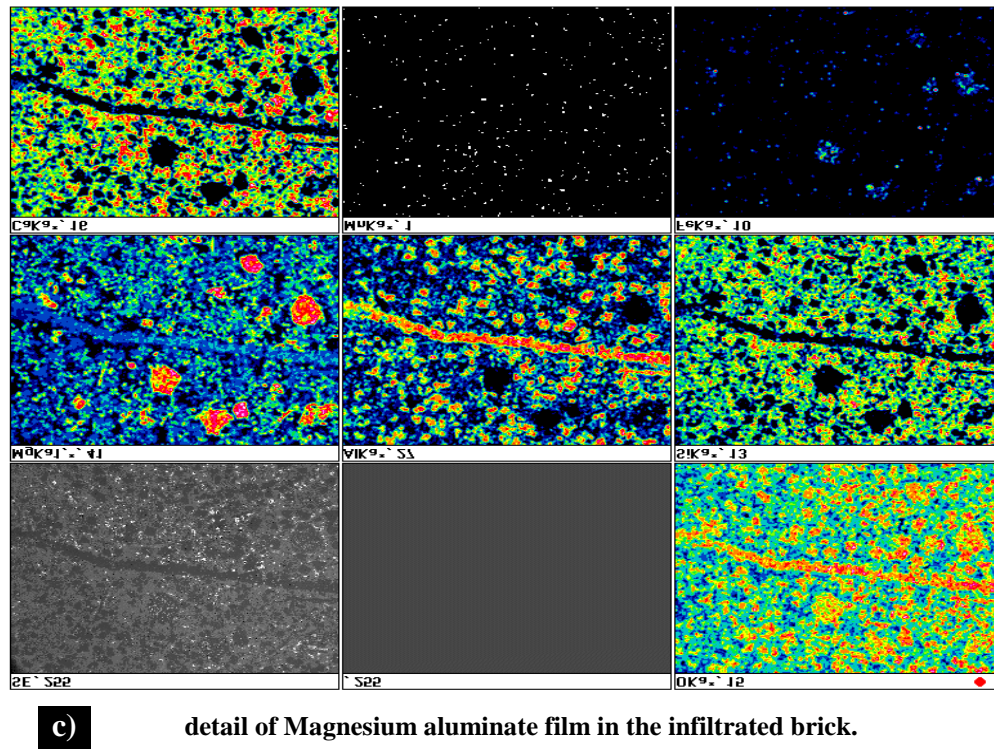


Figure 3c: SEM element distributions of the surface layers.

2.2 Inclined plane tests

In these laboratory experiments, ladle slags were placed on the top of an inclined plane made from the refractory and allowed to flow down the incline in order to simulate the flow of slag in the ladle.

2.2.1 Experimental

The inclined planes (Figure 4) were machined by Vesuvius from MG-1762 grade MgO/10%C refractory (Table 1). There is some decarburization of the refractory surface during the preheating of the ladle; a decarburized surface was produced in these tests by heating several inclined planes in a stainless steel box containing graphite powder in a muffle furnace at 1000°C for 60 minutes. Pressed pellets (15mm diam.) of one of the four slags (Table 2) were placed on the top of the plane. The furnace was then heated to 1600°C and maintained at this temperature for a known period of time. The inclined plane was then removed and subjected to visual and metallographic examination. The depth of slag infiltration was determined by slicing the inclined plane, cutting, mounting and polishing and then examining it in a scanning electron microscope (SEM).

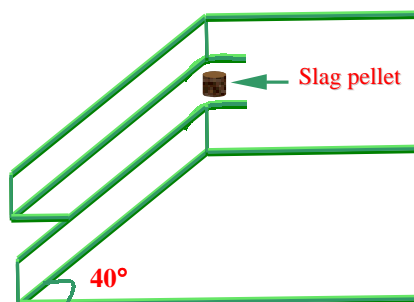


Figure 4: Simple schematic of slag pellets placed on MgO/C refractory inclined plane.

Other tests to study slag infiltration were carried out by placing a pellet of the slag (samples 534 or 466) on a horizontal plaque of either MG-1762 or MGL-37X refractory (the latter having an Al addition of 4.5 %).

Table 1: The composition and physical properties of MG-1762 & MGL 37X refractory bricks.

MG1762	MgO	C (Retained)	SiO ₂	Al ₂ O ₃	Fe ₂ O ₃	CaO	TiO ₂	Mn ₃ O ₄	Cr ₂ O ₃
Composition	96.34	9.8	0.73	0.45	0.34	1.98	0.01	0.08	0.07
MGL37X	MgO	C (retained)	SiO ₂	Al ₂ O ₃	Fe ₂ O ₃	CaO	TiO ₂	Mn ₃ O ₄	Cr ₂ O ₃
Composition	96.8	8.0	0.57	4.5	0.29	1.87	0.01	0.08	0.06

Table 2: Composition of slags used in the present work.

Slag	Met Fe	FeO	CaO	SiO ₂	MgO	Al ₂ O ₃	P ₂ O ₅	MnO	CaS	K ₂ O	V ₂ O ₅	TiO ₂	BaO	Cr ₂ O ₃
438	3.36	1.29	37.3	27.3	13.9	15.2	0.06	3.3	0.17	0.05	0.05	0.28	0.01	0.02
466	3.43	3.86	31.9	23.4	12.7	8.9	0.06	16.7	0.21	1.8	1.8	0.47	0.00	0.08
534	1.8	2.20	31.3	30.8	15.2	12.3	0.05	6.0	0.17	0.04	0.04	0.56	0.14	0.02
566	3.9	3.54	37.4	27.2	16.1	11.2	0.11	4.4	0.36	0.18	0.18	0.39	0.01	0.04

2.2.2 Results and Discussion

The flow properties of the different slags in the inclined plane tests indicated that slags 534 and 466 flowed readily over the refractory plane whereas slags 438 and 566 did not flow significantly. Several tests were carried out and the results were consistent

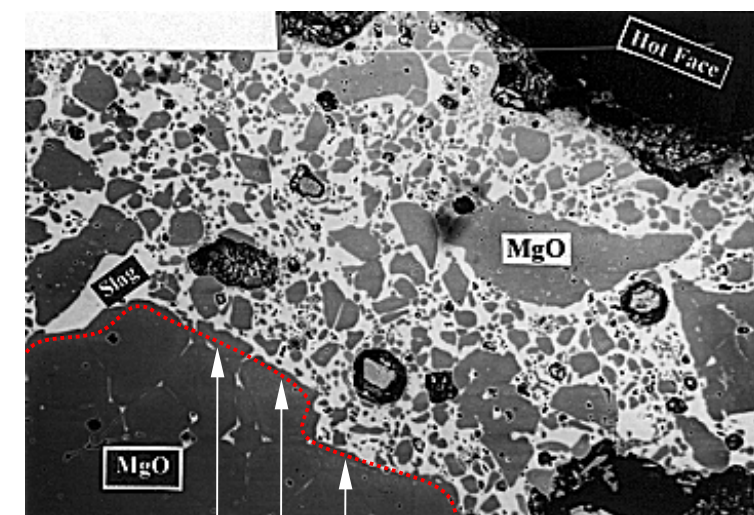
The low fluidity of slags 438 and 566 was attributed to either the fact that (i) these slags had high viscosity or (ii) that they contained phases with high melting points. The latter

explanation was preferred since it was consistent with other observations on these slags. Furthermore, the calculated viscosities derived from the chemical composition using various models reported in the literature [7-9] show no large differences in viscosity (Table 3). However, liquidus temperatures for all four slags, as calculated by the Gaye model, showed values between 1440 and 1460°C, well below the furnace temperature of 1600°C. It was concluded that slags 438 and 566 either contained high melting phases or had been contaminated with MgO when the glaze was removed from the refractory wall.

Table 3: Comparison between measured and calculated values.

Viscosity [Mpas] based on BS-TTC analysis												
Temperature	1673K				1773K				1873K			
Method	Meas	R	U3	KTH	Meas	R	U3	KTH	Meas	R	U3	KTH
Slag												
438	--	180	517	388	--	106	299	201	--	66	184	112
466	--	61	243	391	--	41	152	221	--	29	100	132
534	310	205	476	430	159	126	278	228	94	81	172	129
566	--	97	348	351	--	64	207	187	--	44	134	106
Meas = measured values, R = Riboud Model, U3 = Urbain III Model and KTH = the KTH model												

The depth of slag penetration was measured using the horizontal plaque test samples. A typical example is shown in Figure 5 and it can be seen that penetration depths tend to be variable and consequently an averaged value (I) was obtained.



Red dotted line shows the slag infiltration limit.

Figure 5: Photograph showing irregular slag (534)infiltration into MG-1762 refractory.

The average penetration depth, l , was determined as a functions of (a) holding time (b) slag type and (c) refractory type. It was found (i) that l did not vary with holding time (ii) that slag 534 penetrated deeper than 466 and (iii) that penetration was 10% deeper in refractory MGL 37X than in MG 1762, which was surprising since the latter had a slightly higher porosity. However, the experimental uncertainty in the measurement of l could be >10%.

An examination of the micrographs indicated that the slag penetration occurred by the following mechanism;

- (a) flow of slag through the capillaries(i-e, the pores) in the decarburized zone.
- (b) Slow dissolution of the large MgO particles in the slag.
- (c) Further penetration then occurs by the slow process of slag attack at the grain boundaries, these contain calcium silicates arising from the impurities in the magnesia and the graphite.

Thus it is not surprising that l is apparently not greatly influenced by time (between 5 and 30 mins). Both the mechanism proposed and the findings outlined above are consistent with those reported by other workers [10-13].

3 Characterisation of Ladle Slags

Sebring and Franken [5] derived equations for the thickness of the glaze, δ , and the depth of the infiltrated slag layer, l :

Thin Film Theory	$\delta = \sqrt{\frac{3 \eta v_z}{\rho g}} = \sqrt[3]{\frac{3 \eta \phi_v}{\rho g b}} \quad (1)$	
------------------	--	--

Landau-Levich Theory	$\delta = 0.944 \left(\frac{\gamma}{\rho g} \right)^{1/2} \left(\frac{\eta v_z}{\gamma} \right)^{2/3} \quad (2)$	
----------------------	--	--

Slag Penetration Theory	$l = \sqrt{\frac{\gamma d \cos \theta}{2 \eta}} t \quad (3)$	
-------------------------	--	--

Where, δ = film thickness [m]; ϕ_v = volume flow [m^3/s]; v_z = average velocity [m/s]; ρ = density [kg/m^3]; η = viscosity of slag [$Pa \cdot s = kg/m \cdot s$]; b = outline, inside ladle wall [m]; γ = interfacial tension (slag/gas) [N/m]; l = penetration depth [m]; d = pore diameter [m]; θ = contact angle between refractory and slag [$^\circ$]; t = contact time [s].

Thus it is apparent from these relationships that the properties (such as viscosity, density and surface tension) of the slag do affect the thickness of the glaze and the depth of penetration. Thus it is necessary to characterise the properties of the ladle slags.

3.1 Liquidus temperatures, T_{liq}

The liquidus temperatures for slags 466 and 534 were determined by differential thermal analysis (DTA). The values of T_{liq} obtained are compared with the estimated values calculated by the Gaye model [14] below:

Slag Designation	T_{liq} (Measured)-°C	T_{liq} (Calculated)- °C
466	1375	1400
534	1390	1456

The samples used in DTA are small and thus the composition of the DTA sample may not be representative of the bulk. Nevertheless, it is apparent that the model provides reasonable estimation of the liquidus temperature.

3.2 Viscosity

The viscosity of slag 534 was determined by the rotating cylinder technique using a Brookfield RD DV III viscometer with molybdenum crucibles and bobs and an argon atmosphere. The results are shown in Figure 6 where they are compared with values calculated using various published models.

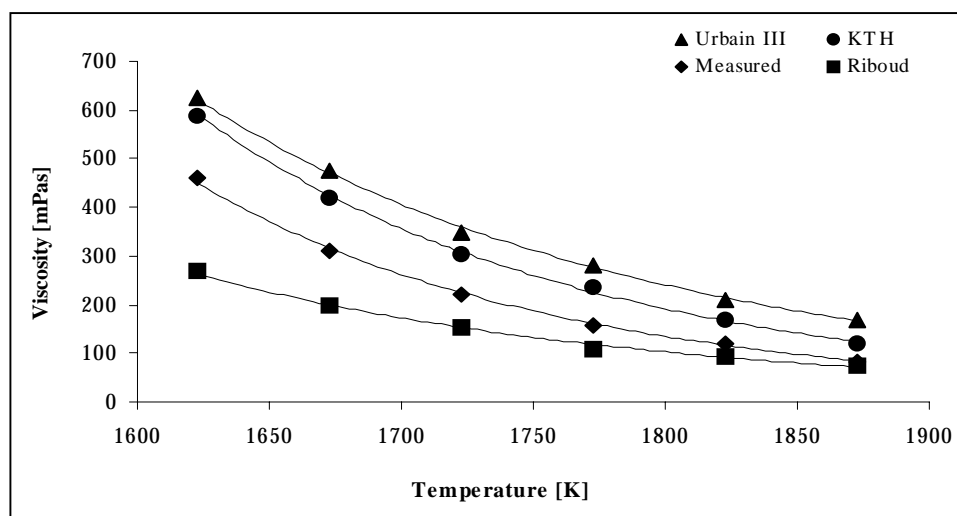


Figure 6: Measured and calculated viscosity values for slag 534.

4 Interfacial Properties

The adhesion of the slag to the refractory is obviously affected by the interfacial properties of the refractory/metal/slag system and the removal of the glaze from the refractory wall almost certainly involves these properties also. Inspection of Equations 2 and 3 indicate that the thickness of the slag glaze, δ , and the depth of slag penetration, l , both involve the surface tension of the slag γ , and slag penetration also involves the contact angle, θ .

4.1 Slag/ metal interfacial tension

It has been shown [15] that in periods of rapid mass transfer the interfacial tension can decrease almost to zero. Thus if mass transfer, such as desulphurization, is still occurring between the steel and the ladle slag it is possible that the interfacial tension is very low and this may have an effect on the adhesion of the slag.

Consequently, the slag/metal interfacial tension was measured in the X-ray sessile drop apparatus at the Royal Institute of Technology, Stockholm. A cube of steel (0.2% C, 0.3% Si, 1.4% Mn, 0.041% Al and 40 ppm S) weighing 4.2 g was placed in an alumina crucible and covered with slag 534. The crucible was then heated to 1570°C and the contours of the molten steel drop in the liquid slag were then monitored, Figure 7. Low interfacial tensions were not observed in this experiment, a value of 609 mNm⁻¹ was derived for the drop shown in Figure 7.

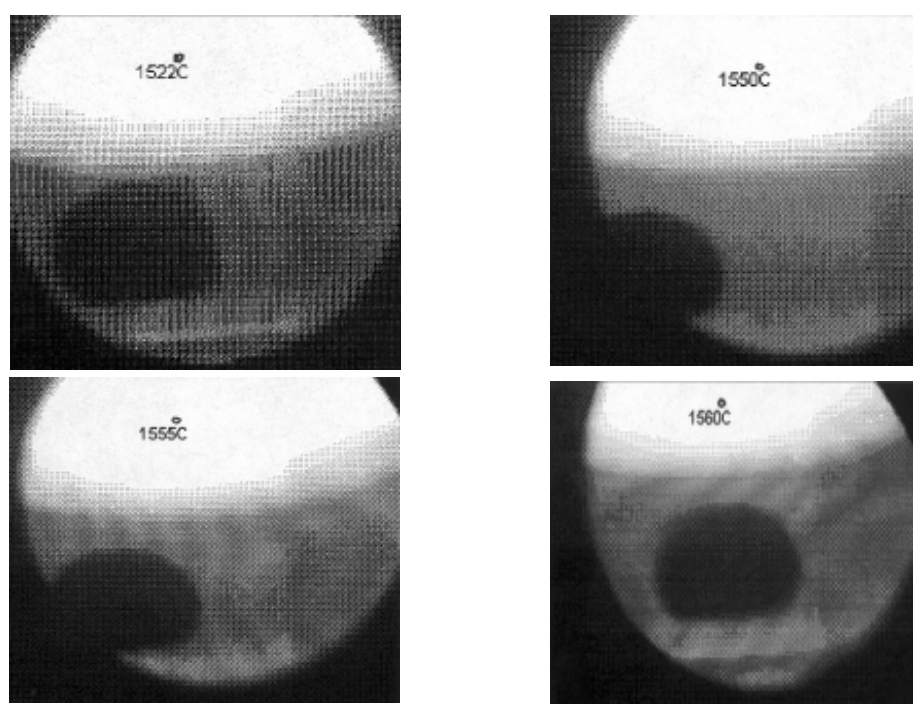


Figure 7: Successive X-ray pictures of a steel sessile drop emerged in slag.

4.2 Slag /refractory contact angle

Attempts have been made to determine the contact angle of slag 534 on a decarburized MgO/C refractory but slag continued to soak into the pores of the refractory and no contact angle could be determined.

4.3 Electrocapillary effects

Kazakov et al. [16] reported that the vertical infiltration of slag into the pores of a refractory could be significantly reduced by increasing the surface tension of the slag; this was done by applying an electrical potential. Their results are shown in Figure 8 and it can be seen that the penetration was at a minimum at ~ -1 volt. Subsequently, Kazakov et al. [16] reported that refractory lifetimes could be increased by a factor of 10 by the application of a small electrical potential between the refractory and the slag. Ladle slag penetration into the refractory could obviously be reduced in this manner but it is also possible that the thickness of the glaze might also be affected by the application of an electrical potential. A thinner glaze would result in a fewer inclusions in the steel. Consequently tests have been carried out to check the findings of Kazakov et al.

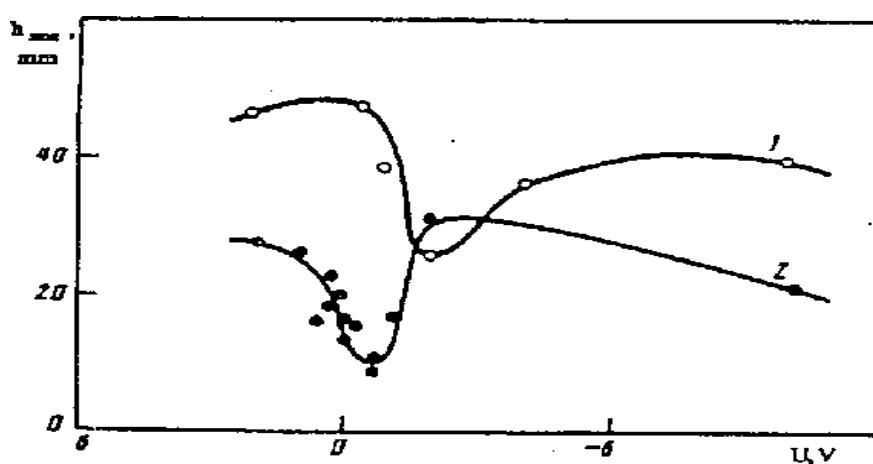


Figure 8: Maximum infiltration of slag in MgO refractory rod (1 - 7mm dia., 2 - 4mm dia.) as a function of electric potential after Kazakov [16].

4.3.1 Experimental

The test was carried out using a decarburized mould flux since it had a low melting temperature. The slag was held in a Pt crucible. The refractory samples were fabricated from two different refractories:

1) Cylindrical samples (10mm diameter and 100mm height) of 96.5 wt% MgO supplied by Vesuvius, UK.

2) Rectangular samples (100mm×6mm) of 98.5 % MgO.

The apparatus used is shown in Figure 9. The slag was brought to constant temperature and then the rod was lowered until it was immersed 2 mm into the molten slag. An electrical potential was applied between the sample and the crucible and the voltage was monitored continuously for the 10 minutes duration of the experiment. A series of experiments at different voltages was undertaken for both refractory samples listed above. The measurements were carried out in air.

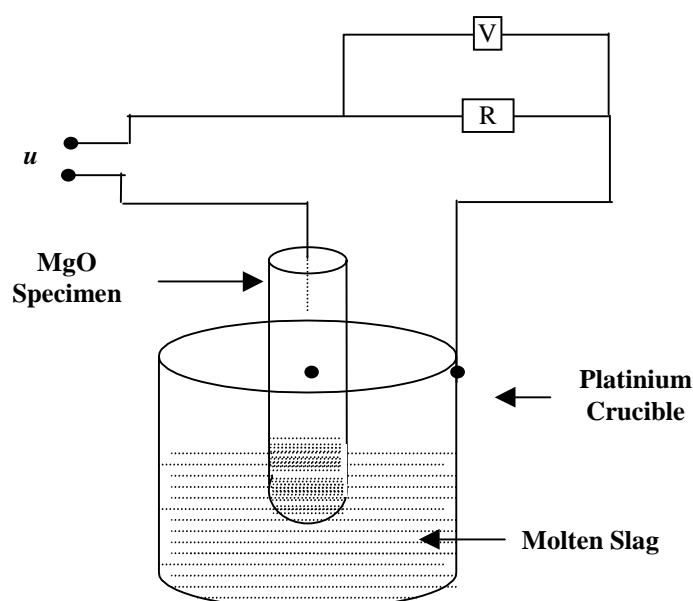


Figure 9: Schematic of electro-cappilarity experiment.

The depth of slag penetration was determined by slicing the refractory specimens longitudinally and then cutting the sliced specimens into appropriate lengths of ~40mm, mounting and polishing and then examining them in an optical microscope to determine the boundary of the slag penetration.

4.3.2 Results and Discussion

The results obtained with the round and square rods are given in Figures 10 a and b respectively. It was also noted that the slag crept up the outside of the specimens, the distance covered is shown as a function of the applied voltage in Figure 11.

Inspection of these figures indicated that :

(i) The results obtained in the present study are identical to those reported by Kazakov et al.

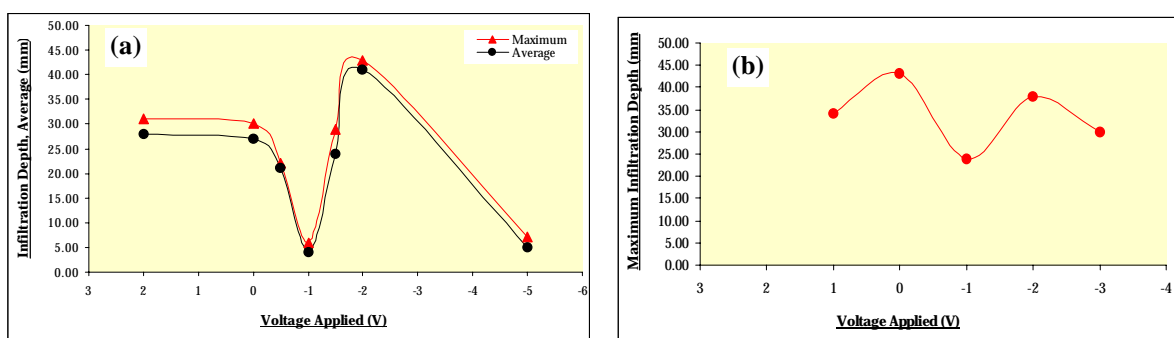


Figure 10: Slag infiltration height for (a) round and (b) square MgO refractory samples as a function of applied voltage.

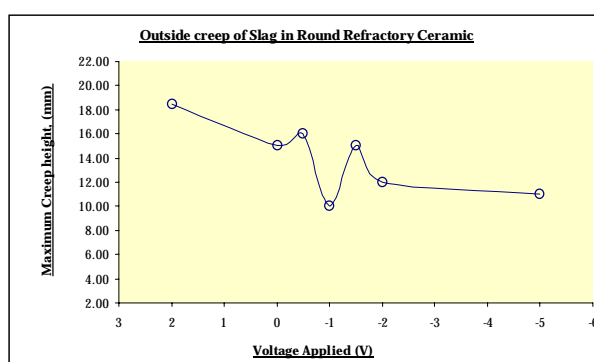


Figure 11: Outside height of round refractory samples covered with slag as a function of applied voltage.

and show that there is a distinct minimum in slag penetration at -1 volt due to the increase in surface tension of the slag under these conditions (this was confirmed in sessile drop experiments of a slag on a Pt. Plate which showed that the contact angle and surface tension were at a maximum when -1 to -2 volts was applied).

(ii) The creep of slag up the outside of the tube shows the same trends as the penetration up the interior of the outside of the tube

Thus there seems that there is a strong possibility of minimising slag penetration into a ladle refractory by applying a small electrical potential.

5 Ladle Glazes as a Source of Inclusions

There is no direct proof that glazes are a prime source of inclusions in steel but it is known that if you want a very clean cast then you must start with a new ladle. Consequently, we have carried out laboratory experiments to show that glazes are a major source of inclusions. These

laboratory tests have been carried out to simulate the formation and removal of the glaze in the ladle as closely as possible.

5.1 Experimental

Crucibles (50mm ID and 40mm high) were machined from MG-1762 (MgO/10%C) refractory by Vesuvius technical centre. Two slags were prepared by mixing and melting weighed amounts of the constituent oxides in a high temperature muffle furnace at 1500°C. The target compositions were given in Table 4.

Table 4: Target composition of Barium free and Barium containing slags.

	CaO	SiO₂	Al₂O₃	MgO	BaO
Slag1	37.5%	37.5%	10.0%	15.0%	----
Slag 2	20.0%	30.9%	8.2%	12.3%	28.8%

The procedures used are illustrated in Figure 12. The same procedures were adopted for the tests with both slags 1 and 2, above and required the use of two muffle furnaces, denoted A and B. The steps involved in this experimental set-up are as follows.

- (i) The crucible was preheated at 1200°C for 1 hour in furnace A whilst slag 1 was melted in furnace B.
- (ii) The crucible was removed from A, placed upside down on a burner flame to keep the interior hot and iron was melted at 1500°C in a graphite crucible placed in A.
- (iii) The crucible was placed upright on a graphite collector (crucible) and an iron "penny " was inserted into the drainage hole.
- (iv) The molten iron was then removed from A and poured into the crucible and then the slag from B was poured on top of the molten iron. and the whole assembly was placed back into furnace A at 1500°C and left for 20 minutes to allow the metal and slag to drain out of the crucible into the collector, thereby forming a glaze in the upper crucible.
- (v) The glazed crucible was placed above another MgO/C crucible (collector) and an iron penny was placed in the hole of the upper crucible. The molten iron was poured into the crucible and then the whole assembly was placed into A at 1500°C and left for 20 minutes.
- (vi) The assembly was then removed from the furnace and allowed to cool and then the metal slug was removed from the collector and 2mm was surface ground from the metal sample to eradicate any slag contamination of the surface.

(vii) The sample was then melted by cold crucible levitation (CCL) to bring any inclusions to the surface of the resultant button.

(viii) These inclusions, derived from the glaze, were then examined in a SEM and their chemical compositions identified by EDX qualitative analysis.

These experiments were then repeated with the slag doped with BaO (slag 2).

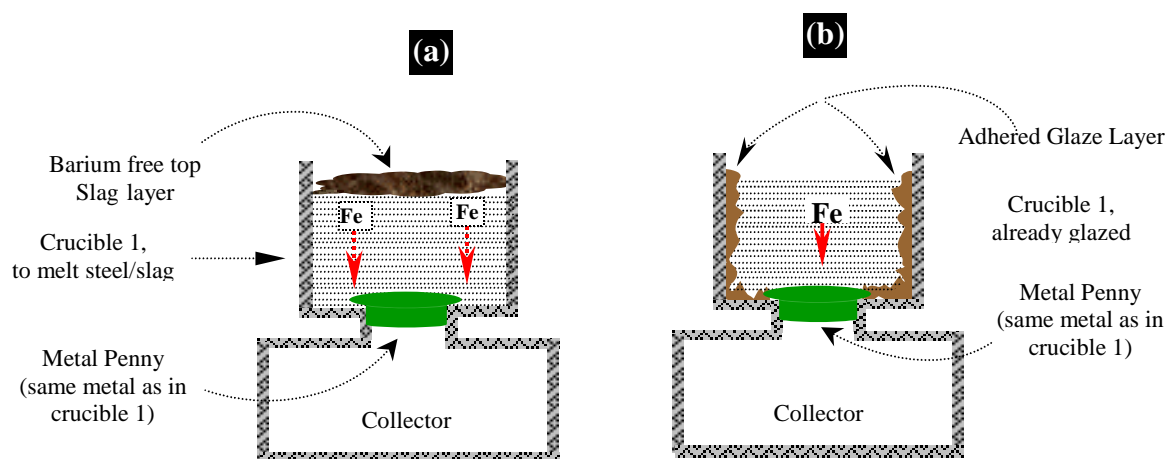


Figure 12: Schematic illustrating the steps involved in doping trial experiments.

5.2 Results and Discussion

The surfaces of the CCL buttons of the steels derived in the presence of glazes for the BaO-doped and un-doped slags were examined and the chemical compositions determined using EDX. Figure 13 shows micrographs for the doped and un-doped steels. The chemical analysis of the inclusion particles is shown in Figure 14. It can be seen that some of the inclusions from the "doped" tests contained significant levels of BaO whereas there was no traces of BaO found in any inclusions produced in the un-doped trials. This observation provides a strong evidence for the fact that inclusions in the steel emanate from the ladle glaze since the only source of BaO was the glaze and the inclusions derived from the un-doped glaze were totally free from BaO. Furthermore, the removal of the outer 2mm of the steel means that the inclusions could not have emanated from the direct contact with the glaze. Consequently, these results provide strong and direct evidence for the ladle glaze being a major source of inclusions.

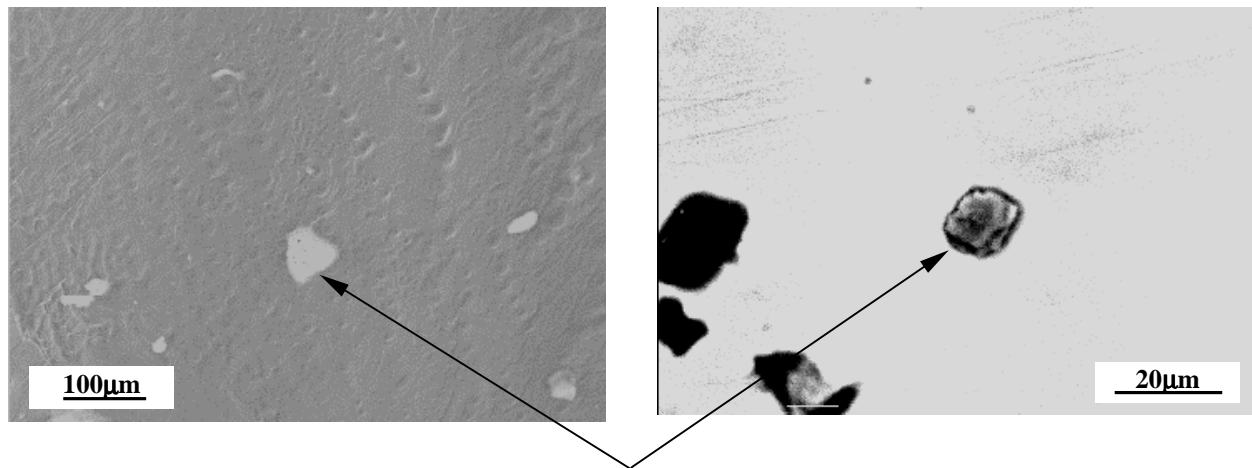


Figure 13: SEM backscattered electron images showing the presence of Barium containing inclusions (arrowed) in metal melted in glazed crucible of Barium doped slag.

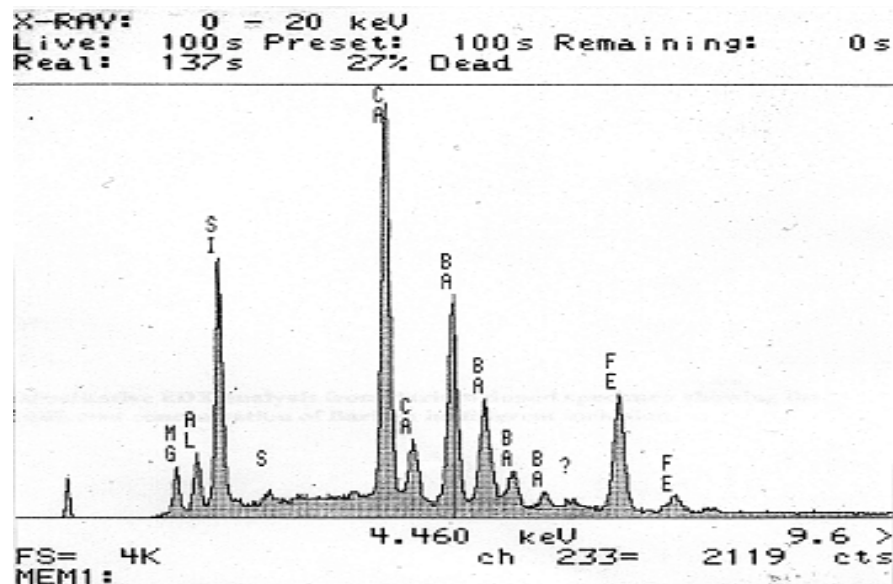


Figure 14: Qualitative EDX analysis from Barium doped specimen showing the presence of different concentration of Barium in different inclusion.

6 Conclusions

- 1: This work has shown unequivocally that ladle glazes are a major source of inclusions in the final product.
- 2: Slag penetration into the refractory occurs rapidly by slag infiltration through the pores created in the decarburized region of the hot face of the MgO/C but further penetration is slow and occurs by infiltration down the grain boundaries.

3: It has been confirmed that slag penetration into refractories can be minimised by the application of an electric potential of –1 volt.

Acknowledgements

Authors wish to thank Dr John Quin and Vesuvius for the very valuable discussion and material, and Robert Ericsson (KTH-Stockholm), Ariel Chang, Alex Karam, Serene Teo, Melvin Andrews for their help with the experimental work and Dr Peter Quested (NPL) for his advice on cleanness evaluation.

References:

- [1]: Hassall, GB; Bain K: Corus-Group, Teesside Technology Centre, Grangetown, Middlesbrough, UK, unpublished results (1996).
- [2]: Shinada N.: Taikabutsu 28 (1976) 371-374.
- [3]: Predergast I D: “Practical aspects of refractory selection and performance in steel ladle – Part 2”; Iron and Steelmaker (1982) 18-22.
- [4]: van Wijngaarden JNVT: Proc. Electric Arc Furnace (1991), 361-367.
- [5]: Seibring R, Franken MC: Glazing of steel ladles; Proc. 5th int. conf. Held Aachen, 1996.
- [6]: Pietorius E, Marr R: The effect of slag modelling to improve steelmaking processes, Proc. 53rd Electrical furnace Conf. Orlando, FLA, 1995.
- [7]: Riboud P, Lucas LD: Canad. Met. Q.20 (1984) 179.
- [8]: Urbain G et al: Steel Research 58 (1987), 111-115.
- [9]: Seetharaman S, Du Sichen, Zhang JY: J Metals, 51(8), 1999, 18
- [10]: Lee WE and Zhang S: Int. Materials Review, 44(3), 1999, 77-104
- [11]: Evans D & Quin J; Metals & Materials, May 1990, 290-292.
- [12]: Pickering GD and Batchelor JD; Ceramic Bulletin, 50(7), 1971, 611-614.
- [13]: Horio T, Fukuoka H and Asano K; Taikabutsu Overseas, 6(1), 1986, 11-15.
- [14]: Gaye H et al: Revue de Metallurgie (1987), 759.
- [15]: Gaye H, Lucas LD, Olette M, Roboud PV: Can. Met Quart. 23(1984), 179.
- [16]: Kazakov A A, Matveev Y V, Arykova L A and Ryabov V V: Russian Metallurgy No.4, (1993).